VIP Colloidal Particles Very Important Paper

DOI: 10.1002/anie.201406136

Reconfigurable Swarms of Nematic Colloids Controlled by Photoactivated Surface Patterns**

Sergi Hernàndez-Navarro, Pietro Tierno, Joan Anton Farrera, Jordi Ignés-Mullol, and Francesc Sagués*

Abstract: *Different phoretic driving mechanisms have been proposed for the transport of solid or liquid microscopic inclusions in integrated chemical processes. It is now shown that a substrate that was chemically modified with photosensitive self-assembled monolayers enables the direct control of the assembly and transport of large ensembles of micrometer-sized particles and drops that were dispersed in a thin layer of anisotropic fluid. This strategy separates particle driving, which was realized by AC electrophoresis, and steering, which was achieved by elastic modulation of the nematic host fluid. Inclusions respond individually or in collective modes following arbitrary reconfigurable paths that were imprinted by irradiation with UV or blue light. Relying solely on generic material properties, the proposed procedure is versatile enough for the development of applications that involve either inanimate or living materials.*

In the emerging field of microfluidics, analytical operations are usually performed by pumping chemicals through channels that are typically hundreds of micrometers wide.[1] For integrated lab-on-a-chip devices, the ability to transport femtosized volumes of solid[2] or liquid[3] chemical cargo without relying on permanent geometrical constraints is required. Colloidal suspensions, which are formed by microsized inclusions embedded in a carrier fluid, are a natural starting point for such a strategy. The self-assembly of colloidal entities can be tuned by controlling the inclusion size[4] and shape,[5] surface chemistry,[6] or by suspending the colloids in a structured liquid.[7]

Different strategies exist to drive and steer individual colloids that are dispersed in a liquid,[8] although the control and large-scale addressability of collections of motile inclusions has proven challenging to realize. With holographic optical traps, direct control over the placement of a few hundreds of inclusions is possible,[8a] although the technique is limited by the field of view of the optical system. Reconfigurable colloidal clusters can be achieved through the interplay of phoretic and osmotic mechanisms,[9] which has opened new perspectives for self-assembly[10] and dynamic transport of inclusions[11] or swarms.[9b,12]

Of particular interest is the use of alternating current (AC) electric fields, which avoid the ion migration mechanisms that are caused by direct current driving. Whereas individual metallodielectric Janus particles can be driven by this method in aqueous media,[13] AC electrophoresis can be used with nematic liquid crystal (NLC) hosts[14] to transport solid[15] or liquid inclusions.[16] A NLC is an oil that features long-range orientational order (the director field) of its constituent molecules, but can also be formed in concentrated aqueous suspensions of amphiphiles (lyotropic liquid crystals).[14] One of the most intriguing characteristics of these viscoelastic materials is their interaction with non-flat surfaces, in particular colloidal inclusions, which leads to the proliferation of topological point and line defects. This interaction can result in colloid-based self-assembling materials[17] and be used as a positioning mechanism for embedded colloids.[18]

We integrated all of the above possibilities into a novel electro-optical technique that permits to remotely address the reversible assembly and collective transport of micrometer-sized colloidal inclusions of arbitrary shape and composition, both solid and liquid, that are dispersed in a thin NLC film. We used liquid-crystal-enabled electrophoresis (LCEEP)[15b] to propel the colloidal inclusions embedded in the NLC cell and a photosensitive anchoring layer to modify the local director field, which, in turn, sets the direction of the colloidal motion. We assembled or disassembled swarms and controlled their placement and motion over arbitrary paths on a surface.

Our system consisted of a NLC film that was inserted between parallel glass plates coated with a transparent electrode, which allowed the application of electric fields perpendicular to the plates. One of the plates was functionalized with a photosensitive self-assembled azosilane monolayer, so that an alternation between perpendicular (homeo-

[*] S. Hernàndez-Navarro, Prof. J. Ignés-Mullol, Prof. F. Sagués
Department of Physical Chemistry, Universitat de Barcelona
Martí i Franquès 1, 08028 Barcelona, Catalonia (Spain)
E-mail: jignes@ub.edu
Dr. P. Tierno
Department of Structure and Constituents of Matter
Universitat de Barcelona
Avinguda Diagonal 647, 08028 Barcelona, Catalonia (Spain)
Prof. J. A. Farrera
Department of Organic Chemistry, Universitat de Barcelona
Martí i Franquès 1, 08028 Barcelona, Catalonia (Spain)
S. Hernàndez-Navarro, Dr. P. Tierno, Prof. J. A. Farrera, Prof. J. Ignés-Mullol, Prof. F. Sagués
Institut de Nanociència i Nanotecnologia, Universitat de Barcelona
Martí i Franquès 1, 08028 Barcelona, Catalonia (Spain)

[**] We thank Patrick Oswald for the polyimide compound. We acknowledge financial support by MICINN (FIS2010-21924C02, FIS2011-15948-E) and DURSI (2009 SGR 1055). S.H.-N. acknowledges support through an FPU Fellowship (AP2009-0974). P.T. further acknowledges support from the ERC through the starting grant "DynaMO" (335040) and from the "Ramon y Cajal" program (RYC-2011-07605).

Supporting information for this article is available on the WWW under http://dx.doi.org/10.1002/anie.201406136.

tropic) or planar (tangential) boundary conditions (anchoring) of the contacting NLC is possible. The counter plate was treated with a spin-coated polyimide compound to achieve strong and permanent homeotropic anchoring. Without external influences, these boundary conditions led to uniform homeotropic anchoring of the NLC. By irradiation with UV light (365 nm) from an incoherent source, we forced the azosilane monolayer to adopt a *cis* (planar) configuration, which could be easily reverted to a *trans* configuration (homeotropic) with blue light (455 nm; Figure 1, see also the Supporting Information, Figure S1). We employed a NLC with negative dielectric anisotropy, which aligned itself parallel to the glass plates upon application of the electric field. This led to degenerate planar-alignment conditions, as all in-plane orientations for the director field are energetically equivalent, thus enabling the local addressability of the NLC director.

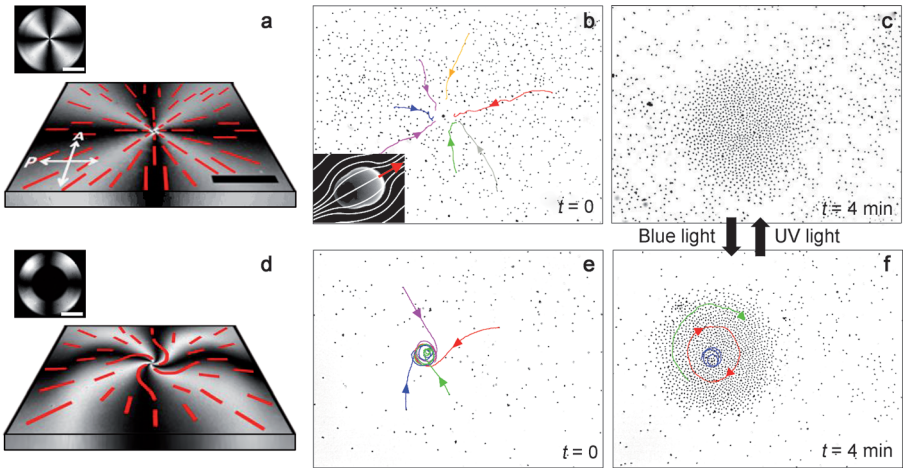

Figure 2. Formation of nematic colloidal clusters. Images (a–c) and (d–f) illustrate the formation of a colloidal aster and vortex, respectively. a, d) Images from a polarized light microscope, obtained with orthogonal polarizer (P) and analyzer (A), of the imprinted NLC texture leading to a cross-like (a) or a spiral (d) attraction pattern. Dashed red lines represent the orientation of the NLC director. Insets: Planar, photoaligned circle (a) and corona (d) prior to application of the electric field. b, c, e, f) Formation of an aster (b, c) and a vortex (e, f) after application of an electric field with a frequency of 10 Hz and an amplitude of 0.87 $V\,\mu m^{-1}$. The trajectories of several particles were superimposed on the images to illustrate the cluster formation mechanism. The inset in (b) shows the SEM image of a single pear-shaped particle ($3\times4\ \mu m^2$), with the NLC field lines and the direction of motion. The colloidal aster in (c) and the vortex in (f) can be interconverted by suitable irradiation procedures, as explained in the text. Scale bars: 200 μm, except for the two insets (500 μm).

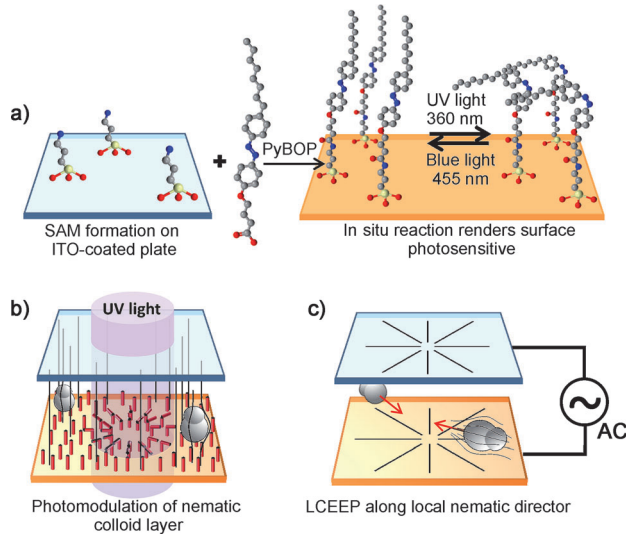

Figure 1. Preparation of photo-addressable nematic colloids. a) Two-step surface-functionalization method to prepare a glass surface coated with photosensitive ITO. The grafted alkyl-azobenzene chains can be reversibly switched between the *cis* and *trans* isomers. b) Colloids are dispersed in a nematic liquid crystal confined between a photosensitive and a non-photosensitive plate. Therefore, patterns of in-plane alignment can be reversibly inscribed with light (here, a circular spot characterized by a radial pattern). The embedded anisometric particles are aligned by the local nematic director (black lines). Upon application of an AC electric field (c), the planar regions expand, and the particles are electrophoretically driven along the local director.

Pear-shaped microparticles made of polystyrene, a material that promotes the planar orientation of the NLC on the particle surface, were used as colloidal inclusions (Experimental Section and Section S1). The chosen particle shape guaranteed a dipolar component in the configuration of the local director field, a requirement for LCEEP to be an efficient propulsion mechanism. Earlier studies of this mechanism have employed spherical solid[15a] or liquid[16] inclusions, relying on the surface functionalization to achieve homeotropic anchoring on the particle surface, which led to a dipolar arrangement of the NLC director around the inclusion. However, homeotropic anchoring has the disadvantage that it can be transformed into a director configuration with quadrupolar symmetry for which LCEEP propulsion is not effective. Our choice thus ensured that all particles in a large ensemble were similarly propelled.

In the absence of irradiation or an electric field, particles will be oriented perpendicularly to the cell plates, following the uniform NLC director. Irradiating the cell with a UV light spot for a few seconds (Figure S2) forced the NLC that was in contact with the azosylane-treated surface to adopt a planar configuration. As shown in Figure 2a and Figure S3, this configuration conforms to the applied irradiation (Figure S6) by locally adopting a splay (radially-spread) texture organized around a central defect.[14] Application of an external AC field forced the bulk NLC to adopt the splay configuration, which now extended for several millimeters, well beyond the size of the irradiated spot, owing to the anchoring degeneracy. The induced configuration is stable for days in an AC field, which well exceeds the half-life for thermal relaxation of the azosilane film, which is about 30 minutes (Figure S7).

The region with radial alignment will be the basin of attraction for dispersed particles, which tumble instantaneously following the NLC director so that their long axis lays, on average, parallel to the cell plates (Figure S3). Simultaneously, LCEEP sets the particle into motion at a constant speed. This feature allows, for instance, to decouple NLC realignment and particle motion, as their speed is negligible for field frequencies above 50 Hz, whereas NLC realignment can be achieved even with frequencies in the kHz range and above.[14] All particles move according the local NLC director, with roughly half of them being attracted by the photoinduced radial defect and half of them being repelled by it. This is a consequence of the random 90° tumbling of the particle dipole from its initial orientation, perpendicular to the planar alignment induced by the AC field (Figure S4). As shown in Figure 2b,c (see also Movie S1), particles follow the NLC field lines and assemble into a growing aster (star-like) configuration where they jam and come to rest.

We could easily switch the assembly mode between a confined aster and a rotating vortex cluster by taking advantage of the elastic properties of the dispersing NLC and the fact that the particles have to follow the NLC director field. This is achieved by erasing the central region of an imprinted UV area with a smaller spot of blue light, which enforces the *cis* to *trans* isomerization leading to homeotropic NLC alignment.

As shown in Figure 2d and the inset, upon application of the AC field, the planar alignment in the resulting circular corona is extended both outwards and inwards. The region surrounding the inner defect now features degenerate planar anchoring conditions; therefore, it relaxes from the pure splay texture to the less energy-demanding bend (rotational) texture.[19] As a consequence, particles follow spiral trajectories and assemble into a rotating vortex, preceding around the central defect with a constant linear velocity, as seen in Figure 2e,f (see also Movie S1). The vortex cluster can be transformed back into a confined aster by irradiating the region with a UV light spot. Both assembly modes can thus be reversibly interconverted in real time by photoelastic control (Movie S1).

The reversibility and quick response of the photoalignment layer enables straightforward cluster addressability. A preformed aggregate of arbitrary size, either aster- or vortex-like, can be relocated to a preselected place anywhere within the experimental cell with minimum dismantlement of the cluster structure by changing the location of the UV spot. An example of this process is shown in Figure 3a (see also Movie S2 and Figure S4). After blocking the LCEEP mechanism by increasing the field frequency to above 50 Hz, the center of attraction was translated 600 μm to the right. Once LCEEP had been reactivated, the swarm of particles moved towards the new position developing a leading edge around which the particles assemble. Alternatively, according to the same principle, predesigned arbitrary paths that connect distant locations inside the cell can be imprinted, or circuits with complex topologies can be drawn as a simple way to accumulate colloidal swarms in the irradiated area and to further entrain them collectively, as shown in Figure 3b (Movie S2).

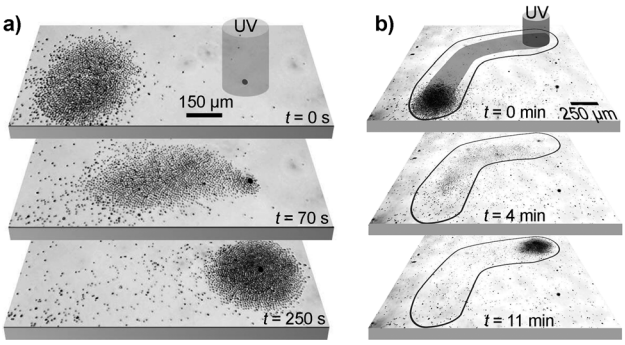

Figure 3. Cluster addressability. Image sequence for a particle swarm traveling across the LC cell because of the in situ reconfiguration of the NLC field. a) The photoaligned spot initially centered with the cluster is moved 600 μm to the right in a straight line, as indicated by the dark spot. b) A longer hybrid track combining curved and straight segments. The contour of the track, only visible between crossed polarizers, is outlined. The applied sinusoidal electric field has an amplitude of 0.74 $V\,\mu m^{-1}$ and a frequency of 10 Hz.

Our strategy to control colloidal aggregation can be readily implemented for the direct or indirect transport of chemical cargo in a channel-free microfluidic environment. For instance, photoactivated lattices of clusters with arbitrary symmetry can be built on an extended surface by imprinting the corresponding distribution of irradiation spots. As an example, a triangular lattice of UV spots was imprinted on the photosensitive surface (Figure 4a; see also Movie S3). Upon application of the electric field, these spots competed as attractors for the particles that were dispersed in the NLC.

Rearrangement of the entire lattice was readily achieved by conveniently reshaping the pattern of projected light spots. We demonstrate this addressability in Figure 4b (Movie S3), where the initially triangular lattice was transformed into a square one. Particle swarms redistribute in the NLC cell according to the new director landscape. Once the electric field had been switched off, the instantaneous cluster pattern was preserved for an extended amount of time. For the used NLC, with a dynamic viscosity of $\eta \approx 0.1$ Pa s, we estimated a self-diffusion coefficient of $D \approx 10^{-3}\ \mu m^2 s^{-1}$. Therefore, it would take several hours for particles of the size used herein to diffuse a few micrometers, and the spontaneous disaggregation of a cluster could take months.

We could also take advantage of our ability to remotely control the dynamic state of an individual cluster to achieve complex mixing patterns in a confined chemical system. As demonstrated for a single aggregate, the state of any site in a lattice can be reversibly switched between a confined aster or a rotating vortex of particles. For example, we show the remote control of just one of the clusters in a square lattice in Figure 4c (Movie S3). The dynamics of this cluster were arrested with a UV light spot, while neighboring clusters remained unaffected. This highlights our ability to selectively address a single swarm and thus to arbitrarily implement complex local mixing patterns.

The reported swarming behavior can be employed to actuate larger embedded objects for which electrophoretic propulsion is not effective. As shown in Figure 5a (Movie S4),

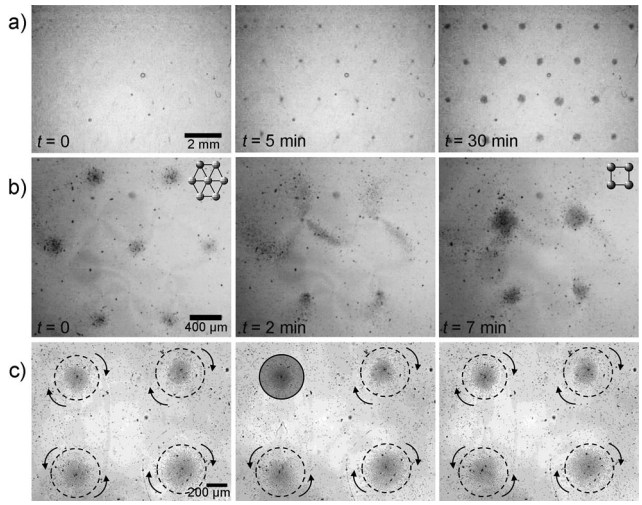

Figure 4. Reconfigurable lattices of clusters. a) Image sequence for the formation of a triangular lattice of particle clusters. A sinusoidal electric field of 0.74 $V\,\mu m^{-1}$ and 10 Hz was used to drive the particles. b) Image sequence for the transformation from a triangular to a square lattice. The original distribution of attractor spots is erased with blue light (455 nm), and a square lattice is subsequently imprinted using UV light (365 nm). The cluster rearrangement occurred when a sinusoidal electric field of 0.78 $V\,\mu m^{-1}$ and 10 Hz was applied. Particle swarms were subsequently formed and redistributed into the reconfigured lattice. c) The dynamic state of the clusters on a lattice can be individually addressed. While all of the clusters were rotating, the dynamics of the top left cluster were first arrested and then restarted again.

a large glass cylinder was set into rotational motion by the collective interaction with the particles in a vortex, which had previously been nucleated on the cylindrical inclusion. The angular speed of the embedded object can be tuned by varying the speed of the driven particles, which is controlled by means of the applied AC field.

Inclusions of any nature are susceptible to being transported using the strategies described here, with the sole requirement being that the NLC director has dipolar symmetry around the colloids. In the case of liquid inclusions, which will spontaneously adopt a spherical shape, the presence of an adsorbed surfactant can be employed to adjust NLC anchoring and to obtain the necessary configuration. In Figure 5b (Movie S4), the controlled aggregation of femtosized volumes of glycerol (stabilized with sodium dodecylsulphate) into an arbitrary spot is shown. Droplets within a designed basin of attraction can be temporarily stored in a defined location for further processing.

The underlying physicochemical mechanisms rely on the generic properties of the involved materials and can be employed to establish complex local mixing patterns or to drive larger embedded objects. Furthermore, as liquid-crystal-enabled AC electrophoresis is also a valid transport mechanism for liquid inclusions, we can envisage an extension of the reported strategy to living systems by employing biocompatible lyotropic liquid crystals.[20] Although biocompatible catalytic micropumps have recently been developed,[21] the perspective of control and addressability offered by our strategy are unparalleled. Finally, and on a broader perspective, the ability to control the dynamic assembly of colloidal inclusions over a surface can lead to novel devices and can be employed to obtain model systems to study swarming behavior or the dynamics of soft active matter.[22]

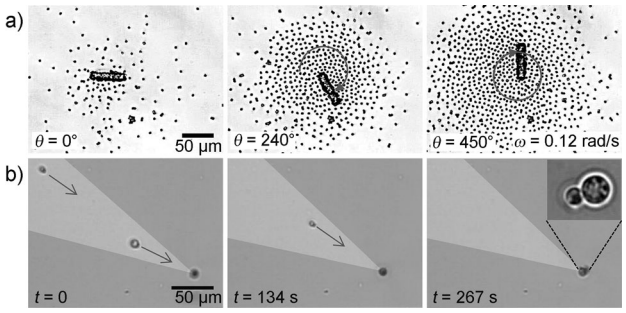

Figure 5. Microfluidic applications. a) A micrometer-sized glass rod (50 μm long, 10 μm in diameter) embedded in a microparticle swarm was set into rotation by the action of the surrounding inclusions. b) Glycerol droplets were accumulated on a spot. Two droplets that were aggregated in this way are shown in the inset.

Experimental Section

Nematic liquid crystal (NLC) cells were prepared using 0.7 mm thick microscope slides with a size of $15 \times 25\ mm^2$, which were coated with a thin layer of indium–tin oxide (ITO) with a sheet resistance of 100 Ω (VisionTek Systems). The plates were cleaned by sonication in a Micro-90 (1%; Sigma–Aldrich) solution, rinsed with ultrapure water (18.2 MΩ cm, Millipore Milli-Q Gradient A-10), and dried at 110 °C for 20 min. To prepare photosensitive plates (Section S1), the ITO surface was first coated with a self-assembled monolayer of (3-aminopropyl)triethoxysilane (APTES, Sigma–Aldrich).[23] The surface was subsequently functionalized with 4-octyl-4′-(carboxy-3-propyloxy)azobenzene (8Az3COOH).[24] The synthesis was performed in a dimethylformamide medium (peptide synthesis grade, Scharlau) through an amide bond formation between the terminal amine group of APTES and the acid group of 8Az3COOH, using pyBOP (>97%, Fluka) as the coupling agent, at a molar ratio of 1:1.25 (8Az3COOH/pyBOP). We recorded UV/Vis spectra to verify the photosensitivity of the resulting azosilane film (Figure S5). To prepare counterplates with homeotropic anchoring, the hydrophilic APTES-coated surfaces were spin-coated with a polyimide compound (0626 from Nissan Chemical Industries, using a 5% solution in the solvent 26, also from Nissan) at 2000 rpm for 10 s, prebaked for 1 min at 80 °C to evaporate the solvent, and then cured for 45 min at 170 °C. A photosensitive and a non-photosensitive plate were then separated by a polyethylene terephthalate film (Mylar, Goodfellow, nominal thickness 13 and 23 μm) and glued together along two sides with the ITO layers facing inwards.

Anisometric polystyrene particles (pear-shaped, $3 \times 4\ \mu m^2$, Magsphere) were dispersed in a nematic liquid crystal with negative dielectric anisotropy (MLC-7029, Merck, room-temperature properties: $\Delta\varepsilon$ (1 kHz) = −3.6, $K_1 = 16.1$ pN, $K_3 = 15.0$ pN). Cells were filled with freshly prepared dispersions by capillary action and sealed with glue.

Irradiation of the samples at wavelengths of 365 nm and 455 nm was performed by means of a custom-built LED epi-illumination setup integrated into an optical microscope. The typical light power density was 0.1 $W\,cm^{-2}$ with a spot size in the sub-millimeter range (Section S2). Sinusoidal electric fields were applied using a function generator and an amplifier. Amplitudes were in the range of 0 to 35 V

from peak to peak, while frequencies for particle motion were in the range of 3 to 50 Hz.

Received: July 23, 2014
Published online: August 19, 2014

Keywords: colloids · electrophoresis · liquid crystals · microreactors · self-assembly

[1] a) E. Kim, Y. Xia, G. M. Whitesides, *Nature* **1995**, *376*, 581 – 584; b) T. Squires, S. Quake, *Rev. Mod. Phys.* **2005**, *77*, 977 – 1026.
[2] L. Baraban, D. Makarov, R. Streubel, I. Monch, D. Grimm, S. Sanchez, O. G. Schmidt, *ACS Nano* **2012**, *6*, 3383 – 3389.
[3] H. Song, J. D. Tice, R. F. Ismagilov, *Angew. Chem.* **2003**, *115*, 792 – 796; *Angew. Chem. Int. Ed.* **2003**, *42*, 768 – 772.
[4] A. Yethiraj, J. H. J. Thijssen, A. Wouterse, A. van Blaaderen, *Adv. Mater.* **2004**, *16*, 596 – 600.
[5] S. C. Glotzer, M. J. Solomon, *Nat. Mater.* **2007**, *6*, 557 – 562.
[6] a) S. Jiang, Q. Chen, M. Tripathy, E. Luijten, K. S. Schweizer, S. Granick, *Adv. Mater.* **2010**, *22*, 1060 – 1071; b) Y. Wang, D. R. Breed, V. N. Manoharan, L. Feng, A. D. Hollingsworth, M. Weck, D. J. Pine, *Nature* **2012**, *491*, 51 – 55.
[7] P. Poulin, H. Stark, T. C. Lubensky, D. A. Weitz, *Science* **1997**, *275*, 1770 – 1773.
[8] a) D. G. Grier, *Nature* **2003**, *424*, 810 – 816; b) W. F. Paxton, K. C. Kistler, C. C. Olmeda, A. Sen, S. K. St Angelo, Y. Cao, T. E. Mallouk, P. E. Lammert, V. H. Crespi, *J. Am. Chem. Soc.* **2004**, *126*, 13424 – 13431; c) W. F. Paxton, P. T. Baker, T. R. Kline, Y. Wang, T. E. Mallouk, A. Sen, *J. Am. Chem. Soc.* **2006**, *128*, 14881 – 14888; d) J. Howse, R. Jones, A. Ryan, T. Gough, R. Vafabakhsh, R. Golestanian, *Phys. Rev. Lett.* **2007**, *99*, 048102; e) J. Wang, *ACS Nano* **2009**, *3*, 4 – 9; f) I. Buttinoni, J. Bialké, F. Kümmel, H. Löwen, C. Bechinger, T. Speck, *Phys. Rev. Lett.* **2013**, *110*, 238301; g) W. Wang, T. Y. Chiang, D. Velegol, T. E. Mallouk, *J. Am. Chem. Soc.* **2013**, *135*, 10557 – 10565; h) W. Gao, A. Pei, R. Dong, J. Wang, *J. Am. Chem. Soc.* **2014**, *136*, 2276 – 2279.
[9] a) W. Duan, R. Liu, A. Sen, *J. Am. Chem. Soc.* **2013**, *135*, 1280 – 1283; b) M. Ibele, T. E. Mallouk, A. Sen, *Angew. Chem.* **2009**, *121*, 3358 – 3362; *Angew. Chem. Int. Ed.* **2009**, *48*, 3308 – 3312; c) J. Palacci, S. Sacanna, A. P. Steinberg, D. J. Pine, P. M. Chaikin, *Science* **2013**, *339*, 936 – 940.
[10] A. Bricard, J. B. Caussin, N. Desreumaux, O. Dauchot, D. Bartolo, *Nature* **2013**, *503*, 95 – 98.
[11] J.-B. Caussin, A. Solon, A. Peshkov, H. Chaté, T. Dauxois, J. Tailleur, V. Vitelli, D. Bartolo, *Phys. Rev. Lett.* **2014**, *112*, 148102.
[12] a) D. Kagan, S. Balasubramanian, J. Wang, *Angew. Chem.* **2011**, *123*, 523 – 526; *Angew. Chem. Int. Ed.* **2011**, *50*, 503 – 506; b) A. A. Solovev, S. Sanchez, O. G. Schmidt, *Nanoscale* **2013**, *5*, 1284 – 1293.
[13] S. Gangwal, O. Cayre, M. Bazant, O. Velev, *Phys. Rev. Lett.* **2008**, *100*, 058302.
[14] P. Oswald, P. Pieranski, *Nematic and cholesteric liquid crystals: concepts and physical properties illustrated by experiments*, Taylor & Francis, Boca Raton, **2005**.
[15] a) O. D. Lavrentovich, I. Lazo, O. P. Pishnyak, *Nature* **2010**, *467*, 947 – 950; b) O. D. Lavrentovich, *Soft Matter* **2014**, *10*, 1264 – 1283.
[16] S. Hernàndez-Navarro, P. Tierno, J. Ignés-Mullol, F. Sagués, *Soft Matter* **2013**, *9*, 7999 – 8004.
[17] a) I. Musevic, M. Skarabot, U. Tkalec, M. Ravnik, S. Zumer, *Science* **2006**, *313*, 954 – 958; b) T. A. Wood, J. S. Lintuvuori, A. B. Schofield, D. Marenduzzo, W. C. Poon, *Science* **2011**, *334*, 79 – 83.
[18] A. Martinez, H. C. Mireles, I. I. Smalyukh, *Proc. Natl. Acad. Sci. USA* **2011**, *108*, 20891 – 20896.
[19] For this material, the bend elastic constant is smaller than the splay elastic constant. Therefore, in the absence of boundary conditions, bend distortions will be favored.
[20] S. Zhou, A. Sokolov, O. D. Lavrentovich, I. S. Aranson, *Proc. Natl. Acad. Sci. USA* **2014**, *111*, 1265 – 1270.
[21] S. Sengupta, D. Patra, I. Ortiz-Rivera, A. Agrawal, S. Shklyaev, K. K. Dey, U. Cordova-Figueroa, T. E. Mallouk, A. Sen, *Nat. Chem.* **2014**, *6*, 415 – 422.
[22] M. C. Marchetti, J. F. Joanny, S. Ramaswamy, T. B. Liverpool, J. Prost, M. Rao, R. A. Simha, *Rev. Mod. Phys.* **2013**, *85*, 1143 – 1189.
[23] J. A. Howarter, J. P. Youngblood, *Langmuir* **2006**, *22*, 11142 – 11147.
[24] J. Crusats, R. Albalat, J. Claret, J. Ignés-Mullol, F. Sagués, *Langmuir* **2004**, *20*, 8668 – 8674.

